Standard Operation Procedure for the IAGOS Capacitive Hygrometer (ICH) (part of IAGOS-CORE-Package 1)

(Version 0: 05 January 2017)

Prepared

by

Herman G.J. Smit

Research Centre Juelich GmbH

Institute for Energy and Climate Research: Troposphere (IEK-8)

D-52425 Juelich , Germany

E-mail: H.Smit@fz-juelich.de

Log of Revisions

Version	published	Reason	Pages affected
0	05.01.2017	Initial release by author	all

Table of Contents

1 Rationale

Water vapour is one of the most important parameters in weather prediction (e.g. *Emanuel et al.*, 1995) and climate research (e.g. IPCC 2013). Water vapour plays a prominent role in the atmospheric energy budget and greenhouse effect (e.g.*Webster,* 1994). Water vapour is the source of clouds and precipitation, while it one of the key drivers for and key tracers of atmospheric transport (*Ludlum,* 1980) As a source of the hydroxyl radical water vapour has a strong influence on the chemistry (i.e., oxidative capacity) of the atmosphere and is crucial in the removal of aerosol particles or water soluble gases through heterogeneous reactions (e.g. *Seinfeld,* 1998). Water vapour is involved in the most prominent climate feedback mechanisms. Climate sensitivity estimates depend critically on radiative feedbacks associated with water vapour, lapse rate, clouds, snow, and sea ice, and global estimates of these feedbacks differ strongly among general circulation models (*Bony et al.,* 2006).

Accurate and intensive monitoring of water vapour is a pre-requisite to identify and quantify the underlying processes in the chemistry and physics of the atmosphere and ultimately improving numerical weather and climate prediction. Particularly, to understand the humidity distributions in the upper troposphere (UT) and lower stratosphere (LS), the most sensitive regions with respect to changes in radiative forcing, is crucial for the further development of global climate models and the improvement of their predictions.

Since August 1994, in the scope of the European project MOZAIC (Measurement of OZone and water vapour by Airbus In service airCraft), regular observations of water vapour have been made between the surface and 12 km altitude from five Airbus A340 passenger aircraft. After 20 years MOZAIC stopped operation at the end of 2014. Light and compact hygrometers with capacitive RH-sensors, so called MOZAIC Capacitive Hygrometers (MCHs), were deployed (Helten et al., 1998). In IAGOS-CORE a modern version of the MCH, the IAGOS Capacitive Hygrometer (ICH), has been developed and is in operation since July 2011.

2 Description of Method

2.1 Equipment

The IAGOS-capacitive hygrometer (ICH) is a compact sensing system developed by Enviscope (Frankfurt, Germany) to measure relative humidity (RH) and temperature (T) in ambient air from high-flying, subsonic aircraft. The ICH (Figure 1) consists of three major components:

(i)   ICH-RH: Rosemount housing as aeronautic inlet system
(ii)   ICH-SC: Sensor carrier with RH- and T sensors
(iii)   ICH-TB: Transmitter box
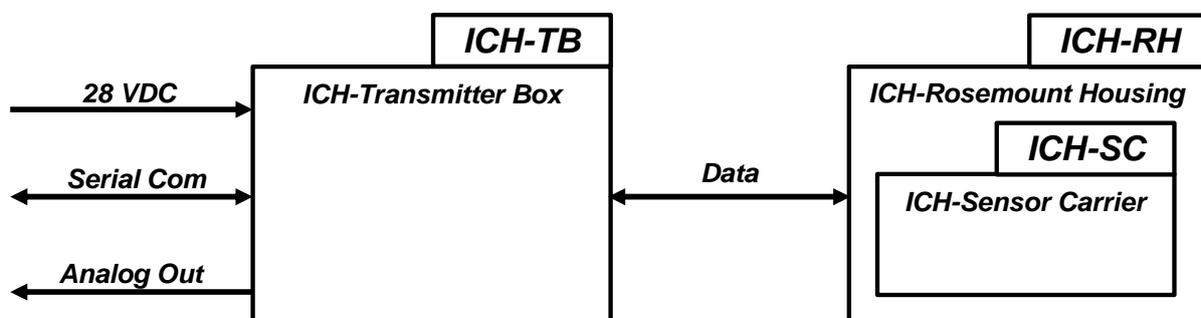

Figure 1   *Schematic layout of IAGOS Capacitive Hygrometer Sensing System (ICH-SS)*

Technical details of ICH-SS are documented in "Declaration of Design and Performance for ICH-SS" (DDP-75423-ICH-SS) issued by enviscope GmbH (Frankfurt, Germany; http://www.eniscope.de).

The ICH-SS (Figure 2) is part of IAGOS-CORE Package 1. The transmitter box (ICH-TB) is mounted on top of the box containing the ozone and carbon monoxide instruments plus the data acquisition system. For further details about installation in the avionics bay see SOP-document of IAGOS-CORE Package 1.
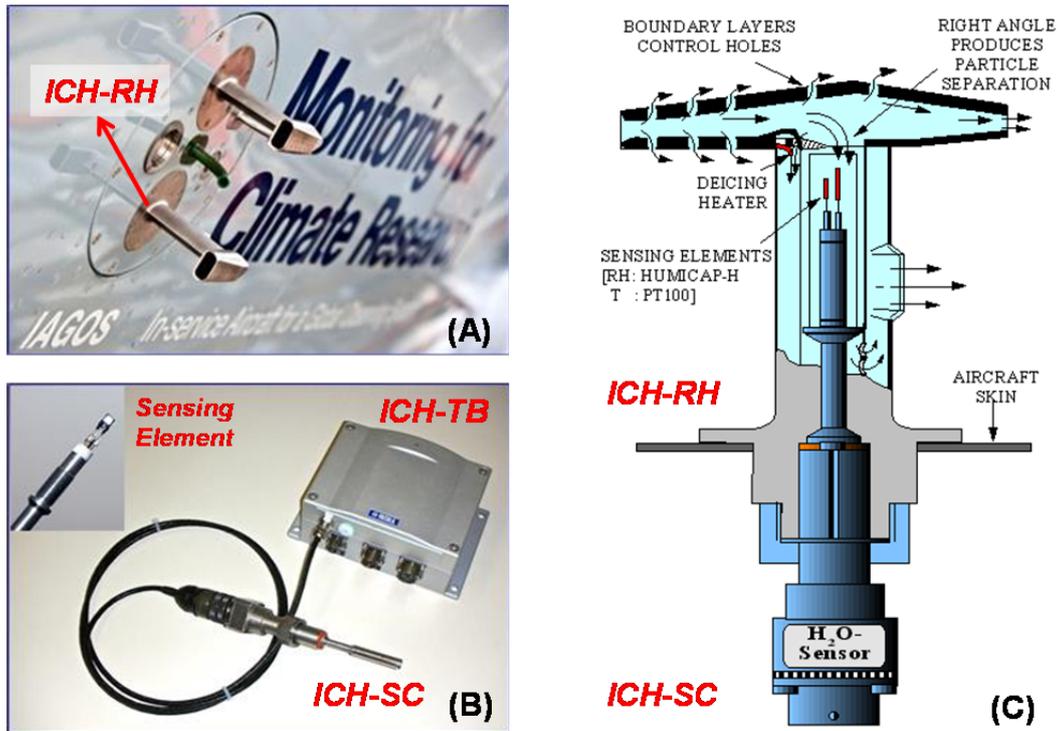

Figure 2 *Left upper photo (A): IAGOS-Inlet plate with ICH-inlet system (ICH-RH= Rosemount housing, Model 102 BX); Left lower photo (B): ICH-sensor carrier (ICH-SC) with sensing elements for relative humidity (Humicap) and temperature (PT100) to be installed in the Rosemount housing mounted on the outside skin of the aircraft. The ICH transmitter box (ICH-TB) is a microprocessor controlled electronic transmitter unit (HMT 333, Vaisala, Finland); Right schematics (C): Cross section of sensor carrier (ICH-SC) mounted in the ICH-RH inlet system.*

The sensing element consists of a capacitive RH sensor (Humicap-H, Vaisala, Finland) plus a PT100-sensor for the direct measurement of the temperature at the humidity sensing surface. Based on thin-film technology the RH-sensor consists of a hydro-active polymer film as dielectric between two electrodes applied on a glass substrate. The sensor responds to changes of relative humidity rather than absolute humidity in the surrounding air. The additional measurement of temperature with the PT100 thermistor enable to derive the absolute humidity using the measured air pressure provided by the aircraft avionics.

The sensing element (Humicap RH-sensor plus +PT100-thermistor) are mounted at the top of an axisymmetric body designed for installation in an appropriate housing (ICH-RH: Model 102 BX, Rosemount Inc., Aerospace Division, USA). The sensor housing (ICH-RH: Figure 2-A) is known to allow accurate measurements of ambient air temperatures (*Stickney et al.,* 1994). The special aeronautic design of the housing protects the sensors against particles and thermal or humidity influences by the walls inside the housing (*Helten et al.,* 1998). The

housing with both sensors is positioned outside the fuselage, 7 m aft of the aircraft nose on the left side just below the cockpit.

The measured humidity and temperature signals are converted into physical units by a microprocessor-controlled transmitter unit (Figure 2-B; ICH-TB: HMT 333, Vaisala, Finland). This unit passes the relative humidity (RH) and temperature (T) signals as voltages to the automated data acquisition system of IAGOS, part of Package 1 of IAGOS-CORE located in the avionics bay of the aircraft.

2.2 Instrument Operation

2.2.1 Temperature Measurement

The air entering the Rosemount housing (ICH-RH) is subject to adiabatic compression caused by the strong speed reduction in the inlet part of the housing that leads to a significant temperature increase of the air flowing past the sensors. The thermal recovery process at the sensing element is well defined (*Stickney et al.*, 1994). In flight, Static Air Temperature (*SAT*) is the temperature of the undisturbed ambient air to be sampled and Total Air Temperature (*TAT*) is the maximum temperature attainable by air when brought to rest. The relation between total and static air temperature is

$$TAT = SAT \cdot \left(1 + \left(\frac{c_P - c_V}{2c_V}\right) \cdot M^2\right)$$
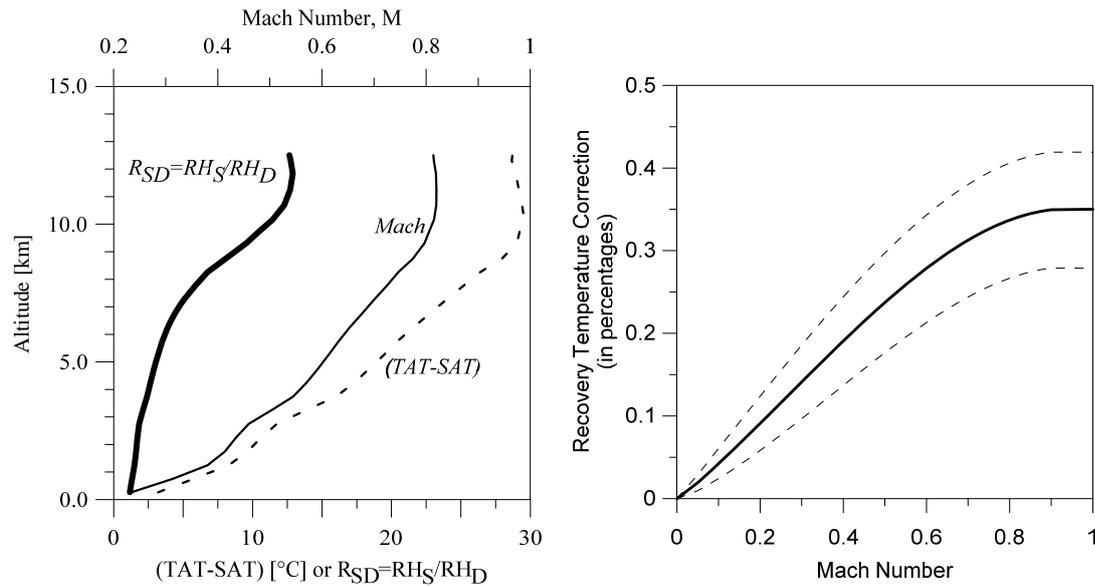(Eq.1)

Figure 3 **Left panel:** *Mean values of the speed of the IAGOS aircraft (Mach number, thin solid line, upper scale) as a function of altitude. The broken line (lower scale) gives the corresponding difference between the temperature measured by the sensor and the ambient temperature (TAT-SAT) and the thick solid line gives the ratio between ambient (static) and measured (detected or dynamic) relative humidity (RHS/RHD).* **Right Panel:** *Recovery temperature correction η (in %) as function of Mach number obtained from wind tunnel data for Rosemount 102 BX model type (source: Stickney et al. 1992).*

In equation (Eq.1), c_p (= 1005 J kg^{-1} K^{-1}) and c_V (= 717 J kg^{-1} K^{-1}) are the specific heats of dry air at constant pressure and volume, respectively, and *M* is the Mach number, i.e., the aircraft speed (relative to air) divided by the speed of sound. *M* is available in flight from the

avionics of the aircraft. For the Airbus A340 *M* typically increases from values of about 0.2 near ground to 0.81±0.01 at cruise altitude (Figure 3 left panel) the resulting difference between total and static air temperature increases from 2K near ground to approximately 30K at 10–12km cruise altitude; see Figure 3 left panel.

The thermal recovery is not exactly 100%. Therefore the temperature measured by PT100 inside the housing, the detected recovery temperature (*DRT*) of the sensing element, is lower than the total air temperature (TAT). The housing manufacturer provides an empirical recovery factor η to determine the *TAT* from *DRT* by the relation

$$TAT = \frac{DRT}{1 - \eta(M)}$$
(Eq.2)

The recovery factor *η*, a function of the Mach number M (Figure 3 right panel), was determined from a series of wind tunnel experiments [*Stickney et al.,* 1994]. Even at large Mach numbers the recovery factor is smaller than 0.004 such that the increases of *DRT* to *TAT* are always smaller than 1 K (Helten et al., 1998)

2.2.2 Relative Humidity Measurement

Because of the strong temperature increase, the relative humidity *RHD* detected by the sensing element in the Rosemount housing is appreciably lower than the static relative humidity of the ambient air, *RH*S(*Helten et al.*, 1998).

$$RHS = \left[\left(\frac{SAT}{DRT} \right)^{\frac{Cp}{Cp - Cv}} \cdot \frac{E_W(DRT)}{E_W(SAT)} \cdot RHD \cdot \right.$$
(Eq.3)

The first factor in Eq.3 describes the adiabatic compression, while the second term accounts for the different water vapour saturation pressures E_W over liquid water at *SAT* and *DRT*, respectively.

For the evaluation of the water vapour data we follow the formulation of E_W by *Goff-Gratch* (1946) over a plane surface of pure liquid water, as recommended by the World Meteorological Organisation (*WMO*, 1983) and adapted to the International Temperature Scale 1990 (ITS-90; *Sonntag,* 1994):

$$E_W(T) = Exp\left[\frac{a}{T} + b + c \cdot T + d \cdot T^2 + e \cdot Ln(T) \right]$$
(Eq.4)

where E_W is in Pa and *T* in K. For a liquid water surface, the constants are:

a = -6096.9385 K, *b* = 21.2409642, *c* = -2.711193E-2 K^{-1}, *d* = 1.673952E-5 K^{-2}, *e* = 2.433502

At a cruise altitude of 10-11 km with a typical SAT of -50 to -60 ^{o}C, *RHD* is a factor of 12-13 lower than *RHS* (Left panel of Figure 3). Therefore, the humidity sensor usually operates within the lowest 10% of its dynamic range. This fact is not adequately covered by the factory calibration provided with the transmitter unit and hence requires frequent individual recalibration of each sensor (*Helten et al.*, 1998), in particular of the sensor bias (*Smit et al.* 2008).

2.3 Instrument Data

During flight the RH and T signals measured by the Humicap and PT100 sensors are collected by the microprocessor controlled transmitter box (ICH-TB) and fed as two analog voltages (0-10V) into the central data acquisition system of package P1 of IAGOS-Core for further digital data control and storage. Every 4 seconds the measured RH & T voltages are stored together with the simultaneously recorded data of the O_3, CO, and BCP (=Backscatter

Cloud Probe) instruments plus a suite of aircraft avionics data (e.g. ambient air pressure, true air speed of aircraft, Mach number, etc.).

3 Maintenance and Calibration

3.1 Maintenance

Approximately every 600-800 hours of flight operation the IAGOS-Humidity Hygrometer (ICH) has to be replaced in order to undergo maintenance and quality-checking procedures including calibration at the laboratory of the Research Centre Jülich (FZJ, Germany) in Jülich (Germany). The logistical and technical procedures to be followed are described in detail in the "ICH-SS Maintenance Manual".

Important is that the three components (see Fig. 2B) are treated as one unit and must be kept together in order to keep the performance of the capacitive humidity sensor stable and reproducible during the entire period between pre- and post-flight calibrations.

Following maintenance steps are performed:

1. Replacement of ICH-unit by aircraft technical staff, shipped via IAGOS maintenance center to FZJ.

2. After receipt of ICH-unit, inspection for mechanical and electrical damage and testing for malfunctions of ICH-SC & ICH-TB (incl. connecting cable) is performed.

3. Post-flight calibration in RH&T simulation chamber at FZJ

4. Refurbishment of the sensor elements: Clean the sensor elements of impurities by rinsing them with three time alternatingly with ethanol (~1 ml) and distilled water (~1 ml), followed by drying the elements in a warm air flow at $120^{o}C$ for about 60 seconds

5. Pre-flight calibration in the simulation chamber at FZJ.

6. Shipping of the ICH-unit via IAGOS-maintenance center to the Airline for installation in IAGOS aircraft for further flight operation.

In rare cases the sensor elements (mounted on the top of the axisymmetric body of the ICH-SC (*Fig. 2-A*) may reveal mechanical damage or malfunctioning. In such cases, post flight calibration is not possible. The sensors will be replaced and cleaned (maintenance step 4) before pre-flight calibration is undertaken.

3.2 Calibration

The IAGOS humidity hygrometers are individually calibrated in the laboratory at the Research Centre Jülich before and after about 600-800 hours of flight operation. These pre- and post-flight calibrations are executed in an environmental simulation chamber (*Smit et al, 2000*; http://www.fz-juelich.de/iek/iek-8/en/expertise/Infrastructure/esf/esf_node.html). Typical in-flight atmospheric conditions of pressure, temperature and relative humidity between surface and 12 km altitude can be simulated (*Smit et al.*, 2000).

A Lyman(α) fluorescence hygrometer (*Kley and Stone*, 1978) is installed in the simulation chamber as a reference instrument for the measurement of low water vapour mixing ratios (1-1000 ppmv) with a relative uncertainty of ±4% (*Helten et al.*, 1998). Above 1000 ppmv a dew/frost point hygrometer (General Eastern, Type D1311R) serves as the reference with an uncertainty of ±0.5 K (*Smit et al.*, 2013). Up to three ICH-units (ICH-CS + ICH-TB) can be simultaneously calibrated. Each ICH-TB is housed in an insulating (T≈20-$30^{o}C$) Styrofoam box to protect it against the low air temperatures (down to $-40^{o}C$) in the simulation chamber. The ICH-sensors are positioned in the centre of the outlet of the duct flow of the chamber to sample the air just after it has passed through the LAH. The 5-10 m/s duct flow is driven by an electrical fan inside the chamber.

The calibration procedures are described in detail in *Helten et al.* (1998). The calibrations reveal that the relative humidity of a calibrated sensor (RH_{Cor}) for a constant temperature T_i can be expressed by a linear relation

$$RH_{Cor}(T_i) = a(T_i) + b(T_i) \cdot RH_{UnCor}(T_i)$$
<div align="right">Eq.(5)</div>

where RH_{UnCor} is the uncalibrated output from an individual sensor, while offset (a) and slope (b) are determined as functions of temperature. At a fixed sensor temperature, three different levels of humidity are set which correspond to typical conditions encountered at the sensing element during in-flight operation in the troposphere.

Calibrations are performed at approximate temperatures of +20°C, 0°C, -20°C, -30°C, and -40°C to derive the temperature-dependent coefficients a and b. The offset *a(T)* and slope *b(T)* coefficients are expressed as continuous functions of temperature by fitting the calibration coefficients *a(T$_i$)* and *b(T$_i$)* obtained at the five different temperatures *T$_i$* , respectively.

In 2016 the reference instruments have been extended with a cryogenic dew/frost point hygrometer (MBW-373 LX) that can measure dew/frost temperatures between -80°C and 20°C with an uncertainty of ±0.1^{o}C. The reference instrument is regularly (ever year) calibrated against a transfer standard at MBW-Calibration (Wettingen, Switzerland; http://www.mbw.ch) that is traceable to primary calibration standards at National Measurement Institutes including PTB (Braunschweig, Germany) and NIST (USA).

4 Data Flow and Uncertainty Assessment

4.1 Data Flow

In flight every 4 seconds the measured RH and T signals are recorded by the data acquisition system of package P1. After each flight at the airport all recorded raw flight data of package P1 are transmitted by GSM to the IAGOS data server at Toulouse (France). Here the data are pre-processed by CNRS/Toulouse. From these pre-processed data the raw RH/T data (voltages) are transferred together with aircraft data (date, time, latitude, longitude, pressure, Mach number etc...), by CNRS to FZJ by Internet.

Data from the pre-and post-flight calibrations of ICHs in the RH/T simulation chamber are processed at FZJ. The results provide the calibration functions of the offsets $a_{pre}(T)$ & $a_{post}(T)$ and slopes $b_{pre}(T)$ & $b_{post}(T)$. The raw ICH flight data are post-flight processed using these calibration functions and validated, including estimated RH-uncertainty and validation flag for each measured data point (see sections 4.2.&and 4.3).

After the post-flight processing the original 4 second data records are extended with the newly corrected and validated RH and T data (*RH&T-Cor*). The header of each flight data file is appended with the version number and date of the post-flight processing, the serial numbers of the specific ICH-SC and ICH-TB flown together, and the dates of the pre-and post-flight calibrations of the ICH. The RH&T-Cor data are then transferred to CNRS where they are added to the IAGOS scientific and instrumental data base

4.2 Calculation of Results

After receiving the RH&T-Raw data the following steps are undertaken for each 4 second data record:

1. Conversion of recorded RH and T sensor voltage signals into physical quantities: (i) uncorrected relative humidity (RHD_{UnCor}) measured by Humicap sensor and (ii) detector recovery temperature (*DRT*) measured by PT100-thermistor.

2. Determination of Total Air Temperature (*TAT*) from *DRT* using Eq.(2), whereby the recovery factor η is an empirical function of Mach number (Fig.3, right panel). The Mach number is provided by the avionics data recording system of the aircraft.

3. Determination of static air temperature (SAT) from *TAT* and *M* using Eq.(1)

4. Determination of corrected relative humidity RHD_{Cor} measured by Humicap at *DRT* from the pre- and post-flight calibration functions of the offsets $a_{pre}(DRT)$ & $a_{post}(DRT)$ and slopes $b_{pre}(DRT)$ & $b_{post}(DRT)$:

$$RHD_{Cor}(DRT) = a_M(DRT) + b_M(DRT) \cdot RHD_{UnCor}(DRT) \qquad \text{(Eq.6)}$$

whereby:

Mean offset: $\qquad a_M(DRT) = \left(\dfrac{a_{pre}(DRT) + a_{post}(DRT)}{2} \right) \qquad$ (Eq.7-A)

Mean slope: $\qquad b_M(DRT) = \left(\dfrac{b_{pre}(DRT) + b_{post}(DRT)}{2} \right) \qquad$ (Eq.7-B)

5. Determination of corrected (static) relative humidity of the ambient undisturbed air outside the aircraft (RHS_{Cor}) by applying Eq.(3) for RHD_{Cor}, *DRT* and *SAT*.

4.3 Uncertainty Analysis

The analysis of the RH measurements made with the ICH (or previously MCH) instruments is based on the averages of the individual pre- and post-flight calibration coefficients a and b for each interval of 600-800 hours of flight operation. RHS_{Cor} of the ambient air is determined from the measured RHD_{Cor}, *DRT* and *SAT* by Eq.(3). The uncertainty of RHS_{Cor} is deduced by error propagation of the uncertainty of the following parameters (For details see *Helten et al.*, 1998):

I The uncertainty of RHD_{Cor} which is a composite of the following contributions:

    a. Uncertainty of RHD_{UnCor}, which is approximately 0.1% RH

    b. Uncertainties of the pre- and post-flight calibrations against the Lyman-Alpha and Dew/Frostpoint hygrometer which is approximately 5 % of the measured RH reference values

    c. Half of the absolute values of the differences between the pre- and post-flight calibration coefficients, a and b (Eq.(7-A) and Eq.(7-B)).

II The uncertainties of the temperatures

    a. *DRT* (equal to ±0.25°C)

    b. *TAT* (equal to ±0.30°C), derived from *DRT* (Eq.2), whereby the uncertainty of the recovery factor η of the Rosemount probe housing (Fig. 3 right panel) have been included

    c. *SAT* (equal to ±0.5°C), derived from *TAT* and *M* (Eq.1). The contribution of the uncertainty of the aircraft air speed measurement to *SAT* determination is less than ±0.01°C so this source of uncertainty is negligible

A detailed analysis of the individual uncertainty components contributing to the total measurement uncertainty have shown that the major contribution comes from the differences in the pre- and post-flight calibration coefficients a and b (*Helten et al.*, 1998). *Smit et al.* (2008) have shown that the sensor offset drifts are the most dominating contributor to the uncertainty of the measurements, while the sensitivity (slope) is more stable in time. The total uncertainty of RHS_{Cor} for each humidity measurement is on the average about ±5 % RH between the surface and 12 km altitude. This is also confirmed from several in-flight intercomparisons with more advanced hygrometer flown on board research aircraft (*Helten et al.*, 1999; *Neis et al*, 2015-a; *Neis et al.*, 2015-b).

For measurements of stratospheric humidity, where RH_{Liquid} values below 5% prevail, the uncertainty of the MOZAIC humidity sensor is too large for quantitative water vapour measurements because the response time is too slow to equilibrate in the low RH and T environment. Thus, these data require considerable scrutiny in the data analysis.

4.4 Validation and Flagging

QA/QC of processed data through screening and graphical inspection of the data on physical and atmospheric realism. For each RH & T measurement a status and a validity flag is included. At present this QA/QC process is being further developed to achieve more automatization and more objective criteria for screening the quality and reliability of the data. The new QA/QC-screening system will be implemented in 2017. Each *RHS*_{Cor} as well as SAT measurement will be stored at the IAGOS-scientific data base with its measured value, overall uncertainty and a flag scheme with two flags *IF1* and *IF2* giving the state of processing (e.g. validation) and state of reliability respectively (See Table 1) . The Flagging scheme is

Table 1

Flagging scheme for IAGOS-ICH-Data conform conform the IGAS-document "Guidelines to store and archive IAGOS (Core & CARIBIC) data (Version V2.2., June 2015)

Flag Index IF1	IAGOS-State of Processing (e.g. validation)	Comments
0	Raw	
1	Preliminary (=Delayed Mode)	
2	Final (Validated)	

Flag Index IF2	IAGOS State of Reliabilty of Data	WMO Code 0 33 020
0	Good (i.e. acceptable)	Good
1	n/a	Inconsistent
2	Limited (i.e. Questionable)	Doubtful
3	Erroneous	Wrong
4	Not Validated	Not Checked
7	Missing Value	Missing Value

4.5 Some Aspects of In-Flight Performance

4.5.1 *Time Response and Spatial Resolution*

The response time of the Humicap sensor of the ICH (i.e. MCH) increases with decreasing sensor temperature (~1s @ +20°C; ~15 s @ -10°C; ~30 s @ -20°C; ~1 min @ -30°C; ~3 min @ -40°C, due to slowing down of the adsorption/desorption and diffusion of water molecules into the sensor material [*Antikainen and Paukkunen,* 1994]. This means that the resolution of the vertical profile obtained during ascent and descent of the aircraft will vary depending on sensor temperature and climbing/descending rate of the aircraft (50-200 m @ Z=0-2 Km; 200-400 m @ Z=2-8 Km; 400-500 m @ Z>8 Km); 50-100 m @ Z=0-2 Km). At cruise altitude the response time is about 1-3 min such that at a typical horizontal aircraft speed of 250 m s$^-$[1], the horizontal resolution is about 15-50 km (*Helten* et al.)

4.5.2 Ice Supersaturation

In the upper troposphere (Z=9-12 km) a substantial fraction (0.1-0.3) of the RH measurements show supersaturation with respect to ice (e.g. *Gierens* et al., 2000; *Luo et al.*, 2007). This suggests that water vapour in the upper troposphere is often not in thermodynamical equilibrium with the ice phase . Are these high RH measurements artifacts (e.g. evaporation of ice crystals in inlet system due to adiabatic heating) or real atmospheric features?. At cold temperatures it is very unlikely that evaporating ice crystals are a significant error source (Smit et al., 2013). However, in the lower and middle troposphere, at warmer temperatures, RH_{liquid} > 100% is occasionally observed. This artifact is most likely caused by partial or complete evapouration of liquid droplets after entering the Rosemount inlet. In contrast to ice particles, liquid droplets can be atomized into a large number of extremely small, fast evaporating droplets by the strong shear flow forces caused by the strong speed reduction (*Smit et al.*, 2013).

5 Specifications

*Table 1:*Specifications of IAGOS Capacitive Hygrometer-Sampling System (ICH-SS)

Quantity	Value Units	Explanations/Comments
Dimensions	150x183x77 mm3	LxWxH (envelope)
Mounting		a) Transmitter box (ICH-TB) is mounted on top of box of package P1 containing O3 & CO instruments and data acquisition system b) Sensor carrier (ICH-CS) plus Rosemount housing (ICH-RH) as inlet
Mass	2 kg	Transmitter box plus Rosemount housing (ICH-RH) with Sensor carrier (ICH-CS)
Connectors Transmitter box	MS 3122E-8-33 S MS 3122E 10-6 P MS 3122E 12-8 P	Power In RS231 Port Signal voltages of RH- & T-sensors
Power Consumption a.) Transmitter Box b.) Rosemount Housing	a.) 28 VDC (<10W) b.) 115 VAC (270 W)	a.) Signal processing b.) Optional housing can be heated during flight (de-icing)
Ambient temperature transmitter box	-20 to +50 ^{o}C	
Inlet system	TAT-aeronautic housing	Rosemount housing (ICH-RH) Model 102 BX, Goodrich Inc., USA
Measured quantity	RH: Rel.Humidity over liquid water SAT: Temperature	
Method of detection	RH: Capacitive SAT: PT100	Combined Humicap-H & PT100 sensor (Vaisala, Finland)
Precision	RH: ±1 % RHL SAT: ±0.1 K	
Time resolution	4 s	
Calibration	Every 600-800 flight hours	Before and after flight operation in the laboratory under realistic P, T and RH atmospheric flight conditions
Calibration traceability	Primary standards at PTB (Germany) and NIST (USA)	Laboratory at FZJ: MBW-373 LX traceable to secondary standard at MBW-Calibration (Switzerland)
Overal uncertainty	RH : ± 5 % RHL SAT: ± 0.5 K	

6 References

Antikainen, V., and A. Paukkunen (1993), WMO Instruments and Observing Methods Report 57, WMO/TD-No. 558, Geneva, Switzerland

Bony, S., Colman, R., Kattsov, V. M., Allan, R. P., Bretherton, C. S., Dufresne, J. L., Hall, A., Hallegatte, S., Holland, M. M., Ingram, W., Randall, D. A., Soden, B. J., Tselioudis, G., and Webb, M. J. (2006) How well do we understand and evaluate climate change feedback processes?, J. Climate, 19, 3445-3482, doi: 10.1175/jcli3819.1.

Emanuel, K. and Co-authors (1995), Report of the first prospectus development team of the U.S. Weather Research Program to NOAA and the NSF. Bull. Amer. Meteorol. Soc. 76, 1194-1208.

Helten, M., H. G. J. Smit, W. Straeter, D. Kley, P. Nedelec, M. Zöger, R. Busen (1998), Calibration and performance of automatic compact instrumentation for the measurement of relative humidity from passenger aircraft, J. Geophys. Res., 103, 25643-25652.

Helten, M., H.G.J. Smit, D. Kley, J. Ovarlez, H. Schlager, R. Baumann, U. Schumann, P. Nedelec, A. Marenco (1999), In-flight intercomparison of MOZAIC and POLINAT water vapour measurements, J. Geophys. Res., 104, 26087-26096.

IPCC, 2013: Climate Change 2013: The Physical Science Basis. Contribution of Working Group I to the Fifth Assessment Report of the Intergovernmental Panel on Climate Change [Stocker, T.F., D. Qin, G.-K. Plattner, M. Tignor, S.K. Allen, J. Boschung, A. Nauels, Y. Xia, V. Bex and P.M. Midgley (eds.)]. Cambridge University Press, Cambridge, United Kingdom and New York, NY, USA, 1535 pp.

Ludlum, F.H (1980), Clouds and storms: The behaviour and effect of water in the atmosphere, Pennsylvania State University Press.

Marenco, A., V. Thouret, P. Nedelec, H.G.J. Smit, M. Helten, D. Kley, F. Karcher, P. Simon, K. Law, J. Pyle, G. Poschmann, R. Von Wrede, C. Hume , and T. Cook (1998), Measurement of ozone and water vapour by Airbus in-service aircraft: The MOZAIC airborne program, An Overview, J. Geophys. Res., 103, 25631-25642.

Neis, P., H.G.J. Smit, M. Krämer, N. Spelten, and A. Petzold (2015-a), Evaluation of the MOZAIC Capacitive Hygrometer during the airborne field study CIRRUS-III. Atmos. Meas. Tech. 8, 1233–1243. DOI: http://dx.doi.org/10.5194/amt-8-1233-2015.

Neis, P., H.G.J. Smit, S. Rohs, U. Bundke, M. Krämer, N. Spelten, V. Ebert, B. Buchholz, K. Thomas and A. Petzold (2015-b), Evaluation Quality assessment of MOZAIC and IAGOS capacitive hygrometers: insights from airborne field studies, Tellus B 2015, 67, 28320, http://dx.doi.org/10.3402/tellusb.v67.28320

Seinfeld, J.H. (1998), Clouds, contrails and climate, Nature, 391, 837-838.

Smit H.G.J., W. Sträter, M. Helten, and D. Kley (2000), Environmental simulation facility to calibrate airborne ozone and humidity sensors. Jül Berichte Nr 3796, Forschungszentrum Jülich.

Smit, H.G.J., A. Volz-Thomas, M. Helten, H.W. Pätz, and D. Kley (2008), An in-flight calibration method for near real-time humidity measurements with the airborne MOZAIC sensor, J. Atmos. Oceanic Tech., 25, DOI: 10.1175/2007JTECHA975.1, 656–666.

Smit, H., Kivi, R., Vömel, H., and Paukkunen, A. (2013), Thin film capacitive sensors, in: Monitoring Atmospheric Water Vapour, Vol. 10, ISSI Scientific Report Series, Springer, New York, doi:10.1007/978-1-4614-3909-72, 11–38.

Smit, H. G. J., S. Rohs, P. Neis, D. Boulanger, M. Krämer, A. Wahner, and A. Petzold (2014), Technical Note: Reanalysis of upper troposphere humidity data from the MOZAIC

programme for the period 1994 to 2009 , Atmos. Chem. Phys. Discuss., 14, doi:10.5194/acpd-14-18905-2014, 18905-18942.

Sonntag, D. (1994), Advancements in the field of hygrometry, Meteorol. Zeitschrift, N.F. 3, 51-66.

Stickney, T.M., M.W. Shedlov, and D.I. Thompson (1994), Rosemount total temperature sensors, Tech. Rep. 5755, Revision C, Aerosp. Div. Rosemount Inc., Eagan, Minn.

Webster, P.J. (1994), The role of hydrological processes in ocean-atmosphere interactions, Rev. Geophys., 32, 427-476.

World Meteorological Organization (WMO) (1983), Measurement of atmospheric humidity, Guide to Meteorological Instruments and Methods of Observation, 5th ed., WMO Report No.8, pp. 5.1-5.19, Geneva, Switzerland.